

# Synthetic, Structural, Magnetic, and Mössbauer Spectral Study of {Fe[HC(3,5-Me<sub>2</sub>pz)<sub>3</sub>]<sub>2</sub>}I<sub>2</sub> and Its Spin-State Crossover Behavior

Daniel L. Reger,<sup>\*,[a]</sup> Christine A. Little,<sup>[a]</sup> Mark D. Smith,<sup>[a]</sup> Arnold L. Rheingold,<sup>[b]</sup> Kin-Chung Lam,<sup>[b]</sup> Thomas L. Concolino,<sup>[b]</sup> Gary J. Long,<sup>\*,[c]</sup> Raphaël P. Hermann,<sup>[d]</sup> and Fernande Grandjean<sup>[d]</sup>

**Keywords:** Iron / N ligands / Spin crossover / Magnetic properties / Mössbauer spectroscopy

The complex {Fe[HC(3,5-Me<sub>2</sub>pz)<sub>3</sub>]<sub>2</sub>}I<sub>2</sub> (**1**) has been prepared from the reaction of FeI<sub>2</sub> and HC(3,5-Me<sub>2</sub>pz)<sub>3</sub> (pz = pyrazolyl ring) in a 1:2 ratio. The complex is high-spin in both the solid state and in solution at ambient temperature. In the solid state, magnetic susceptibility and Mössbauer spectral studies indicate that samples of the complex that have been crystallized and dried change completely from high-spin to low-spin upon cooling below 195 K, with a substantial two-step thermal hysteresis in the transition. The spin-crossover properties of **1** are sample dependent: powder samples do not change to low-spin at low temperatures. Two crystalline forms of **1** have been identified by X-ray crystallography, one form containing no solvent of crystallization and the other containing solvent. In both, there is only one iron site, with

average Fe–N bond lengths of 2.18 and 2.17 Å, values that confirm that the complex is high-spin. Single crystals of the nonsolvated form shatter at low temperatures whereas single crystals of the solvated form can be cooled to 110 K with no loss of crystallinity and remain fully high spin at this temperature. Crystallographic information: nonsolvated form is triclinic, *P* $\bar{1}$ , *a* = 8.8062(2) Å, *b* = 10.3549(2) Å, *c* = 11.3549(2) Å,  $\alpha$  = 104.0768(10)°,  $\beta$  = 110.2473(10)°,  $\gamma$  = 92.6385(11)°, *Z* = 1; solvated form is monoclinic *P*<sub>2</sub>/c, *a* = 10.3214(5) Å, *b* = 12.7753(7) Å, *c* = 20.1995(11) Å,  $\alpha$  = 90°,  $\beta$  = 97.5380(10)°,  $\gamma$  = 90°, *Z* = 2.

(© Wiley-VCH Verlag GmbH, 69451 Weinheim, Germany, 2002)

## Introduction

The properties of octahedral iron(II) complexes, especially those with an FeN<sub>6</sub> coordination environment, that undergo thermal spin-state crossovers between the high-spin (HS, *S* = 2) and low-spin (LS, *S* = 0) states have been widely investigated.<sup>[1]</sup> In general, iron(II) complexes that are HS in the solid state at room temperature may show a spin-state crossover to the LS electronic state upon cooling, whereas, complexes that are LS at room temperature may show a spin-state transition to the HS electronic state upon heating.<sup>[1,2]</sup>

We have recently reported, by using a combination of NMR, X-ray structural, magnetic, and Mössbauer spectral results, that {Fe[HC(3,5-Me<sub>2</sub>pz)<sub>3</sub>]<sub>2</sub>}(BF<sub>4</sub>)<sub>2</sub> (pz = pyrazolyl ring) shows unusual spin-crossover behavior in the solid

state.<sup>[3]</sup> Even though only one iron site is observed by X-ray crystallography at ambient temperature, the solid abruptly changes from all-HS above 206 K to a 50:50 mixture of HS and LS (in this form the Fe–N bond lengths are reduced by ca. 0.2 Å, as expected<sup>[1]</sup>) below 200 K, the composition of the lower temperature mixed spin-state does not change as the temperature is lowered to 4.2 K. This spin-state crossover is reversible and shows no thermal hysteresis. Herein we report the synthesis, NMR, X-ray structural, magnetic, and Mössbauer spectral studies of {Fe[HC(3,5-Me<sub>2</sub>pz)<sub>3</sub>]<sub>2</sub>}I<sub>2</sub> (**1**), a complex with the same dication as {Fe[HC(3,5-Me<sub>2</sub>pz)<sub>3</sub>]<sub>2</sub>}(BF<sub>4</sub>)<sub>2</sub>, but paired with a different anion, a change that dramatically effects its properties.

## Results and Discussion

### Synthesis and Characterization

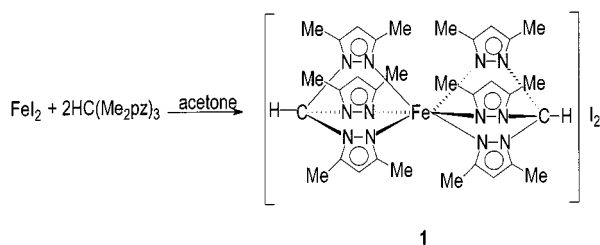
The reaction of FeI<sub>2</sub> and HC(3,5-Me<sub>2</sub>pz)<sub>3</sub> in a 1:2 ratio yields {Fe[HC(3,5-Me<sub>2</sub>pz)<sub>3</sub>]<sub>2</sub>}I<sub>2</sub> (**1**; Scheme 1). FeI<sub>2</sub> is black in solution. Upon addition of the ligand the homogeneous solution immediately becomes yellow and the desired product precipitates as a powder after several minutes. The solid is white as a powder and colorless as single crystals, indicat-

<sup>[a]</sup> Department of Chemistry and Biochemistry, University of South Carolina, Columbia, South Carolina 29208, USA

<sup>[b]</sup> Department of Chemistry and Biochemistry, University of Delaware, Newark, Delaware 19716, USA

<sup>[c]</sup> Department of Chemistry, University of Missouri-Rolla, Rolla, MO 65409-0010, USA

<sup>[d]</sup> Institut de Physique, B5, Université de Liège, 4000 Sart-Tilman, Belgium



Scheme 1

ing that the iron(II) is HS at room temperature.<sup>[1]</sup> The solution <sup>1</sup>H NMR spectrum shows broad resonances shifted over the range from  $\delta = 51.1$  to  $-42.6$ , analogous to that previously reported for {Fe[HC(3,5-Me<sub>2</sub>pz)<sub>3</sub>]<sub>2</sub>}(BF<sub>4</sub>)<sub>2</sub> (**2**), indicating that the complex is also HS in solution.

The HS configuration of the iron(II) in **1** at ambient temperature was verified by the X-ray crystal structures (see Figure 1 and Table 1). Complex **1** crystallizes in two different forms under seemingly identical crystallization procedures. One form of these crystals contains no solvent molecules while the other form contains four molecules of CH<sub>2</sub>Cl<sub>2</sub>, the crystallization solvent, for every iron(II). In both cases, the crystals were found to fragment to microcrystals when taken out of solution. The crystals used for the X-ray structural studies were taken from a container that contained solvent and were immediately coated with an inert liquid.

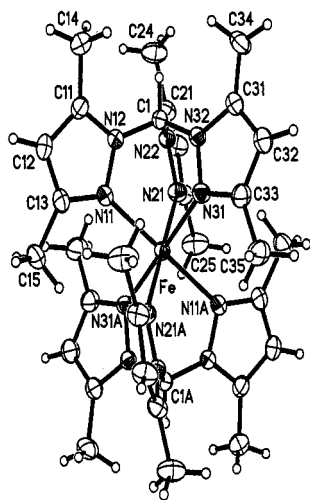


Figure 1. An ORTEP diagram of the cation of the solvated form of {Fe[HC(3,5-Me<sub>2</sub>pz)<sub>3</sub>]<sub>2</sub>}I<sub>2</sub>

The structures of the cations in both forms of **1** are similar (Figure 1) and similar to the cation in **2**, which has been reported previously.<sup>[3]</sup> Table 1 gives selected bond lengths and angles for all of the structures. The average Fe–N bond lengths are 2.18 Å in the nonsolvated form of **1** and 2.17 Å in the solvated form of **1** and in **2**, clearly indicating that iron(II) is in the high-spin configuration at 295 K; average bond lengths of ca. 1.97 Å are typically observed in LS octahedral FeN<sub>6</sub> complexes.<sup>[1]</sup> In all of the structures the iron(II) is located on a center of symmetry and has an N<sub>6</sub>

coordination environment. The chelate rings restrict the intraligand N–Fe–N angles to an average of 84.5° in both forms of **1** and 84.3° in **2**, restrictions that lead to trigonally distorted octahedral structures.

There are important differences in the behavior of crystals of the two forms of **1** and of **2** upon cooling. Crystals of **2** change from colorless above 206 K to purple below this temperature; they also undergo a phase change from monoclinic to triclinic. These crystals, when reheated above 206 K, again become colorless, returning to the monoclinic space group, with no apparent degradation of crystal quality. Crystals of **2** that have been cooled are still suitable for X-ray structural studies at ambient temperature.<sup>[3]</sup> In contrast, crystals of **1** in the nonsolvated form shatter when cooled below 195 K, a temperature below which the solid turns purple. After being cooled, the crystals are no longer suitable for single crystal X-ray studies at either low temperature or after reheating to ambient temperature, at which temperature the sample is again white. Crystals of **1** in the solvated form *do not undergo the spin-state transition* down to 110 K. The quality of the crystals does not change, they remain colorless at 110 K, and there is no phase change at lower temperatures.

There is an interesting and important difference between the structures of the two forms of **1** relating to the degree of tilting of the pyrazolyl rings away from an ideal C<sub>3v</sub> type arrangement. In the absence of tilting, the FeN(n1)–N(n2)–C(n1) torsion angles, where n denotes the ring number, would be 180° and the metal atom would reside in the planes defined by the pyrazolyl rings. We have previously commented on the fact that in octahedral {M[HC(3,5-Me<sub>2</sub>pz)<sub>3</sub>]<sub>2</sub>}<sup>n+</sup> and M[HB(3,5-Me<sub>2</sub>pz)<sub>3</sub>]<sub>2</sub> complexes this ring tilting increases with increasing size of the metal.<sup>[4]</sup> The tilting also changes when the same cation is paired with different anions.<sup>[4]</sup> We have solved the structure of {Fe[HC(3,5-Me<sub>2</sub>pz)<sub>3</sub>]<sub>2</sub>}(BF<sub>4</sub>)<sub>2</sub> (**2**) at 220 K, where all of the cations are HS, and at 173 K, where half of the cations are HS and half LS. In the 220 K structure the torsion angle averages 169°, whereas for the HS form in the 173 K structure this torsion angle averages 162°. For the LS form of the 173 K structure this torsion angle averages 179°, reflecting the smaller size of LS iron(II). For the nonsolvated form of **1**, which changes to LS at low temperatures, this torsion angle averages 171°. In contrast, in the solvated form of **1**, the form that does not change to LS at low temperatures, it is 10° less at 161°.

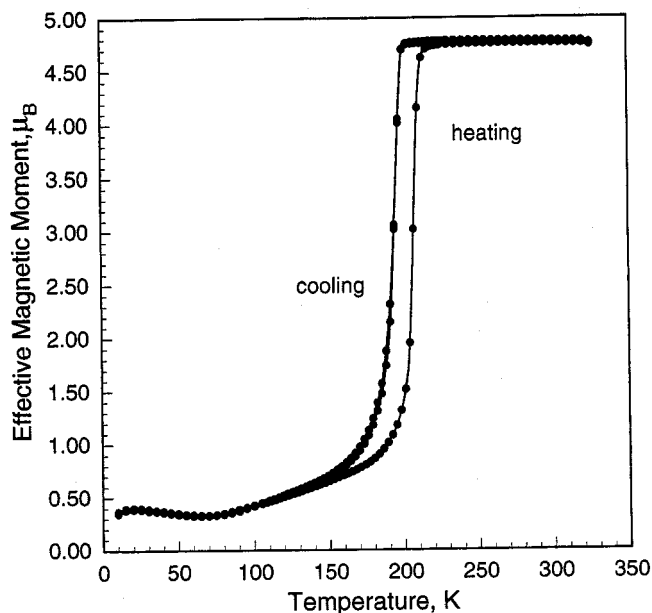
### Magnetic Susceptibility Studies

Both crystalline forms of {Fe[HC(3,5-Me<sub>2</sub>pz)<sub>3</sub>]<sub>2</sub>}I<sub>2</sub> (**1**) discussed in the X-ray section above fragment to microcrystals when dried or if even briefly removed from the crystallization solvents. This process makes it impossible to directly measure the magnetic properties of the single crystals used in the X-ray structural studies.

The effective magnetic moment of a sample originating from the nonsolvated, crystalline form of **1** as a function of temperature between 5 and 325 K is shown in Figure 2. A sample originating from the solvated, crystalline form of **1**,

Table 1. Selected bond lengths and angles for the cation in nonsolvated  $\{\text{Fe}[\text{HC}(3,5\text{-Me}_2\text{pz})_3]_2\}\text{I}_2$ , solvated  $\{\text{Fe}[\text{HC}(3,5\text{-Me}_2\text{pz})_3]_2\}\text{I}_2 \cdot 4\text{CH}_2\text{Cl}_2$  and  $\{\text{Fe}[\text{HC}(3,5\text{-Me}_2\text{pz})_3]_2\}(\text{BF}_4)_2$  (**2**)

Complex	Bond lengths (Å)		<b>2</b>
	Nonsolvated Form	Solvated Form	
Fe–N(11)	2.156(3)	2.157(2)	2.155(3)
Fe–N(21)	2.200(4)	2.174(2)	2.179(2)
Fe–N(31)	2.176(3)	2.171(3)	2.177(2)
C(1)–N(12)	1.443(5)	1.451(4)	1.444(4)
C(1)–N(22)	1.446(6)	1.446(4)	1.451(3)
C(1)–N(32)	1.448(5)	1.447(4)	1.448(4)
Intraligand donor N...N average distance	2.93	2.916(2)	2.91
Distance Fe out of N <sub>3</sub> donor plane	1.371(2)	1.3562	1.373(2)
Bond Angles (deg)			
N(11)–Fe–N(21)	84.49(14)	84.75(9)	84.41(11)
N(11)–Fe–N(31)	83.57(13)	84.11(9)	83.70(10)
N(21)–Fe–N(31)	85.59(14)	84.77(9)	84.67(10)
N(11)–Fe–N(21A)	95.51(14)	95.25(9)	95.59(11)
N(11)–Fe–N(31A)	96.43(14)	95.89(9)	96.30(10)
N(21)–Fe–N(31A)	94.41(14)	95.23(9)	95.33(10)
N(11)–N(12)–C(1)	120.1(3)	119.5(2)	119.2(2)
N(21)–N(22)–C(1)	119.9(3)	119.1(2)	119.6(2)
N(31)–N(32)–C(1)	119.6(3)	120.1(2)	119.8(2)
N(12)–C(1)–N(22)	111.3(3)	111.0(2)	111.4(2)
N(12)–C(1)–N(32)	113.0(3)	111.3(2)	111.9(2)
N(22)–C(1)–N(32)	110.8(3)	111.1(2)	111.1(3)
FeN(11)–N(12)C(11) torsion	168.0(3)	164.2(2)	166.1(2)
FeN(21)–N(22)C(21) torsion	165.9(3)	164.1(2)	168.5(2)
FeN(31)–N(32)C(31) torsion	179.8(3)	157.9(2)	171.4(2)

Figure 2. The effective magnetic moment as a function of temperature, measured by cooling, heating and recooling between 325 and 5 K, of crystallized  $\{\text{Fe}[\text{HC}(3,5\text{-Me}_2\text{pz})_3]_2\}\text{I}_2$  (**1**)

that had been dried and shown by elemental analysis to lose the  $\text{CH}_2\text{Cl}_2$  of crystallization, has essentially the same magnetic properties as shown in Figure 2. At higher temperatures **1** is clearly HS with an effective moment of ca.  $4.8 \mu_{\text{B}}$ , a value that is very close to the iron(II) spin-only value of  $4.9 \mu_{\text{B}}$ . Upon cooling below 195 K there is a dramatic drop in the moment as would be expected for a spin-state crossover to a LS iron(II) complex. Continued cooling to 5 K yields a very small moment, except at the lowest temperatures where a trace of paramagnetic iron(III) impurity leads to a very small increase in the magnetic susceptibility. The low-temperature moment of ca.  $0.4 \mu_{\text{B}}$  is typical of the temperature-independent paramagnetism observed in low-spin iron(II) complexes. Subsequent warming of the sample above 5 K reveals very similar behavior but with the presence of a reproducible hysteresis of ca. 15 degrees in the spin-crossover such that at ca. 210 K, the sample has completely returned to the HS state.

The magnetic properties of complex **1** are dependent on the history of the sample. Figure 3 shows the magnetic behavior of the solid that precipitated from acetone in the original reaction, a sample that is a white powder and is pure as indicated by elemental analysis and NMR spectroscopy. This solid was subsequently used to prepare the crystalline samples, which once dried were used to obtain the

magnetic results shown in Figure 2. For the solid that precipitated from acetone, only a small change in the magnetic moment was observed as the temperature was lowered. The high temperature moment of this sample is the same as observed for both crystallized samples. In contrast, for the sample of **1** that precipitated from acetone, there is only a small decrease in the magnetic moment from  $\mu_{\text{eff}} = 4.85 \mu_{\text{B}}$  at higher temperatures to  $\mu_{\text{eff}} = 4.5 \mu_{\text{B}}$  below 185 K. As with the results presented in Figure 2, a hysteresis of ca. 15 degrees is observed upon cooling and heating for the small changeover. Presumably, the decrease of ca.  $0.4 \mu_{\text{B}}$  is due to the presence of a small amount of microcrystalline **1** that is present in the sample.

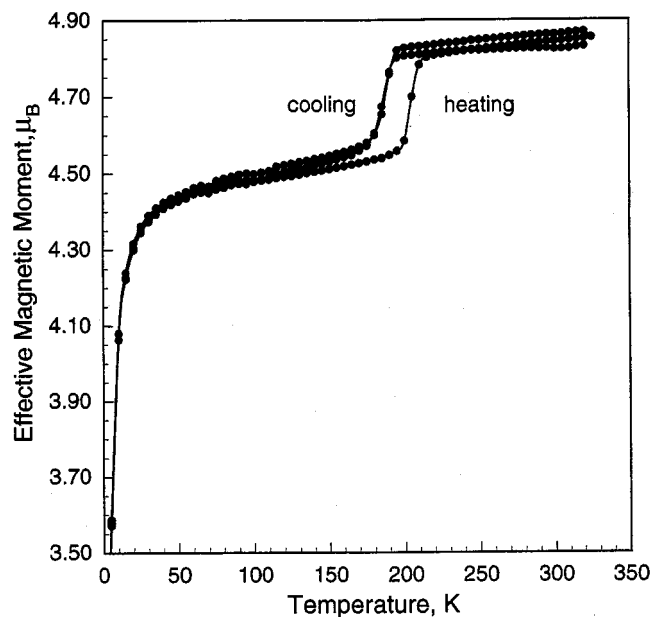


Figure 3. The effective magnetic moment as a function of temperature, measured by cooling, heating and recooling between 325 and 5 K, of a sample of {Fe[HC(3,5-Me<sub>2</sub>pz)<sub>3</sub>]<sub>2</sub>}I<sub>2</sub> that precipitated from the reaction mixture

There is a sharp drop in the effective moment below ca. 30 K (see Figure 3). This drop is not unexpected for a distorted octahedral iron(II) complex in which the low-symmetry component of the crystal field, in conjunction with electron delocalization and spin-orbit coupling, are known<sup>[5]</sup> to lead to a decrease in the observed moments at very low temperatures.

### Mössbauer Spectral Analysis

The Mössbauer spectra of {Fe[HC(3,5-Me<sub>2</sub>pz)<sub>3</sub>]<sub>2</sub>}I<sub>2</sub> (**1**), measured on a sample that was crystallized from CH<sub>2</sub>Cl<sub>2</sub>/hexanes and dried, were obtained upon cooling from 295 to 4.2 K and upon warming from 175 to 215 K (Figures 4 and 5, respectively). Selected hyperfine parameters for this complex are given in Table 2. The complete temperature dependence of the isomer shift and quadrupole splittings for the HS and LS states are shown in Figures 6 and 7. As the sample is cooled, a dramatic change occurs in the spectra starting at ca. 190 K indicating a spin-state crossover from

the HS to the LS state.<sup>[1]</sup> This change is clearly indicated by the appearance of a second doublet at ca. 0.5 mm/s. The change in population of the HS state, as reflected by the Mössbauer spectral absorption area of the HS component, is shown in Figure 8, and matches an analogous plot using data from the magnetic studies.

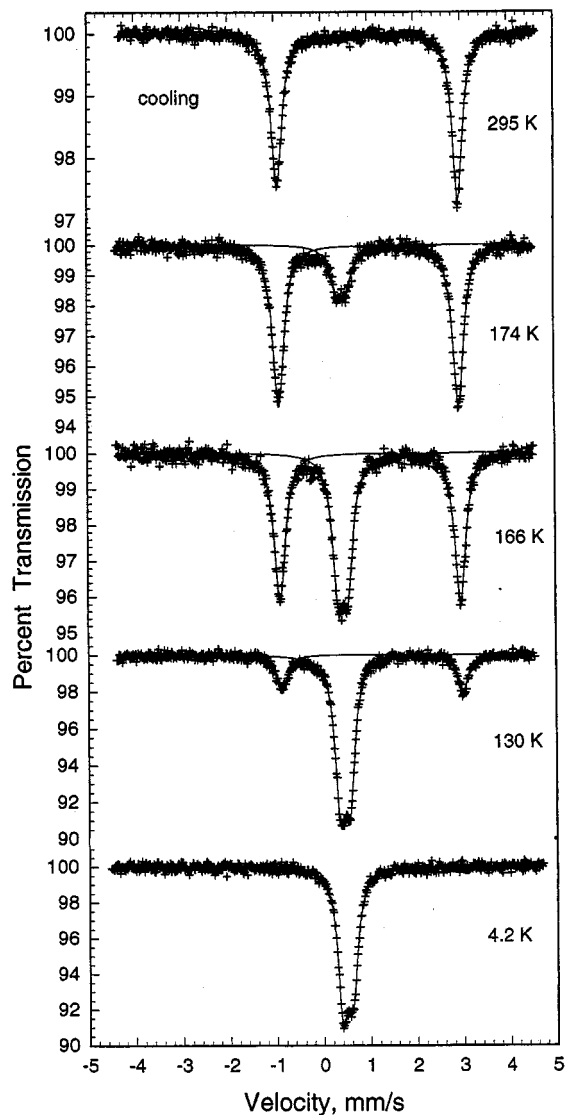


Figure 4. The Mössbauer spectra of crystallized {Fe[HC(3,5-Me<sub>2</sub>pz)<sub>3</sub>]<sub>2</sub>}I<sub>2</sub> (**1**) obtained at the indicated temperatures upon cooling from 295 to 4.2 K

The hyperfine parameters reported in Table 2 are those expected for HS and LS iron(II) complexes with a distorted pseudooctahedral coordination geometry. The isomer shifts and quadrupole splittings for both the HS and LS states of **1** are virtually identical to those of the analogous complex {Fe[HC(3,5-Me<sub>2</sub>pz)<sub>3</sub>]<sub>2</sub>}(BF<sub>4</sub>)<sub>2</sub> (**2**), although the nature of the spin-crossover is different. In **1** the transition to the low-spin state is complete below 70 K but the transition occurs only to 75% in the temperature range from 70 to 150 K on cooling and 70 to 200 K on heating. The presence of a small amount of the HS complex in this temperature range is also

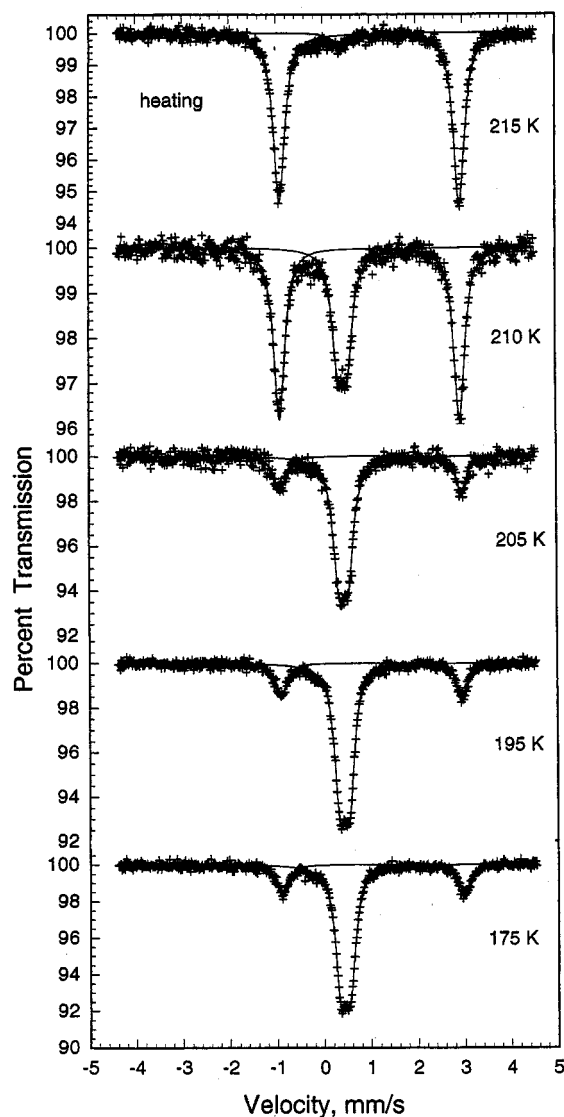


Figure 5. The Mössbauer spectra of crystallized  $\{\text{Fe}[\text{HC}(3,5\text{-Me}_2\text{pz})_3]_2\}\text{I}_2$  (**1**) obtained at the indicated temperatures upon heating from 4.2 K.

apparent in Figure 2 as a shoulder in the effective moment.

A comparison of Figure 2 with Figure 8 indicates that the temperature hysteresis observed in the magnetic measurements is approximately half that observed in the Mössbauer spectral studies. The exact reason for this difference is not apparent at this time, but is probably related to differences in sample preparation. We have shown that thermal equilibrium was achieved in the magnetic studies by stopping the change in temperature at a number of points in both the heating and cooling cycles around 200 K and observing no change of the magnetic moment with time.

Mössbauer spectra were obtained at 90 K and 295 K on the same sample that was used for the magnetic data shown in Figure 3, a sample that precipitated from acetone in the

Table 2. Selected Mössbauer spectral parameters for  $\{\text{Fe}[\text{HC}(3,5\text{-Me}_2\text{pz})_3]_2\}\text{I}_2$  (**1**)

$T(\text{K})$	$\delta$ (mm/s) <sup>[a]</sup>	$\Delta E_Q$ (mm/s)	$\Gamma$ (mm/s)	Relative area (%)	Assignment
295 <sup>[b]</sup>	0.969	3.86	0.28	100	high-spin
190 <sup>[b]</sup>	1.022	3.86	0.30	100	high-spin
180 <sup>[b]</sup>	1.023	3.86	0.27	92	high-spin
	0.432	0.20	0.27	8	low-spin
174 <sup>[b]</sup>	1.029	3.86	0.29	70	high-spin
	0.430	0.19	0.30	30	low-spin
166 <sup>[b]</sup>	1.033	3.87	0.28	57	high-spin
	0.443	0.21	0.27	43	low-spin
130 <sup>[b]</sup>	1.064	3.89	0.28	23	high-spin
	0.459	0.21	0.26	77	low-spin
70 <sup>[b]</sup>	1.095	3.91	0.26	13	high-spin
	0.463	0.21	0.25	87	low-spin
4.2	0.463	0.21	0.26	100	low-spin
175 <sup>[c]</sup>	1.039	3.88	0.28	23	high-spin
	0.440	0.20	0.26	77	low-spin
195 <sup>[c]</sup>	1.012	3.88	0.27	22	high-spin
	0.435	0.20	0.26	78	low-spin
205 <sup>[c]</sup>	1.017	3.87	0.28	25	high-spin
	0.429	0.20	0.27	75	low-spin
210 <sup>[c]</sup>	1.007	3.84	0.28	89	high-spin
	0.418	0.21	0.28	11	low-spin
215 <sup>[c]</sup>	1.010	3.85	0.29	95	high-spin
	0.419	0.20	0.34	5	low-spin
295 <sup>[d]</sup>	1.009	3.90	0.29	100	high-spin
90 <sup>[d]</sup>	1.118	3.92	0.28	85	high-spin
	0.500	0.22	0.25	15	low-spin

<sup>[a]</sup> The isomer shifts are given relative to room temperature  $\alpha$ -iron foil. <sup>[b]</sup> Data obtained on the nonsolvated crystallized sample during the initial cooling from 295 to 4.2 K. <sup>[c]</sup> Data obtained on the nonsolvated crystallized sample after cooling to 4.2 K. <sup>[d]</sup> Data obtained on a powder sample.

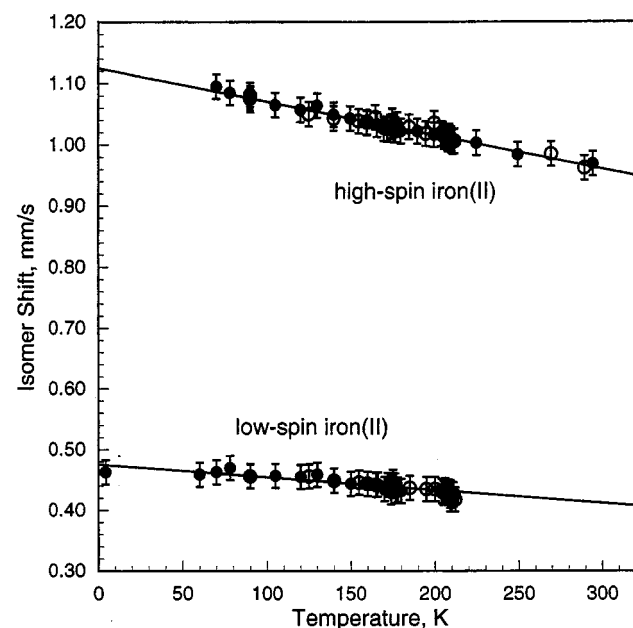


Figure 6. The temperature dependence of the Mössbauer spectral isomer shifts for  $\{\text{Fe}[\text{HC}(3,5\text{-Me}_2\text{pz})_3]_2\}\text{I}_2$  (**1**); the data obtained upon the initial cooling from 295 to 4.2 K are indicated by ● and the data obtained upon the subsequent heating from 4.2 K are indicated by ○.



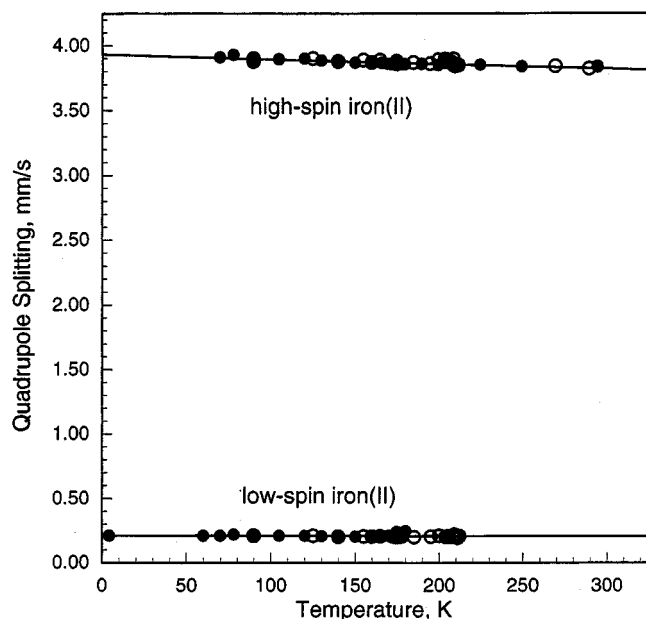


Figure 7. The temperature dependence of the Mössbauer spectral quadrupole splittings for {Fe[HC(3,5-Me<sub>2</sub>pz)<sub>3</sub>]<sub>2</sub>}I<sub>2</sub> (**1**); the data obtained upon initial cooling from 295 to 4.2 K are indicated by ● and the data obtained upon the subsequent heating from 4.2 K are indicated by ○

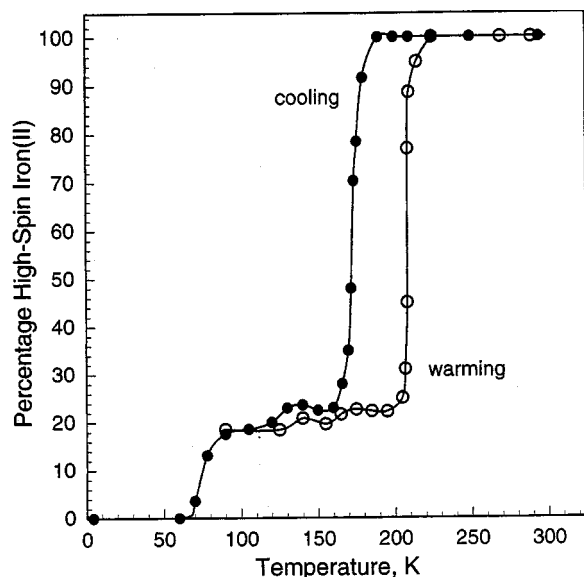


Figure 8. The temperature dependence of the percentage of high-spin iron(II) in {Fe[HC(3,5-Me<sub>2</sub>pz)<sub>3</sub>]<sub>2</sub>}I<sub>2</sub> (**1**); the data obtained upon initial cooling from 295 to 4.2 K are indicated by ● and the data obtained upon the subsequent heating from 4.2 K are indicated by ○

original reaction. At 295 K the sample is fully HS with hyperfine parameters that match those observed with the crystallized samples. At 90 K, only 15% of the sample is LS, approximately the same amount that changes in the magnetic study.

## Conclusions

The most interesting property of {Fe[HC(3,5-Me<sub>2</sub>pz)<sub>3</sub>]<sub>2</sub>}I<sub>2</sub> (**1**) is the temperature-dependent changes in spin-state behavior, changes which are a function of the history of the sample. These changes are observed both in the X-ray diffraction studies carried out on single crystals and in the magnetic and Mössbauer spectral studies carried out on the fragmented microcrystals that form when the single crystals are taken out of solution. Two crystalline forms of **1** have been identified by X-ray crystallography. Although the average Fe–N bond lengths and angles of the FeN<sub>6</sub> cores in the two structures are the same, there are substantial differences in the FeN(n1)–N(n2)–C(n1) torsion angles. In the structure of the nonsolvated form of **1**, measured at 298 K, this torsion angle averages 171°. These crystals shatter when cooled below 195 K, a temperature below which the solid turns purple, indicating a change to the LS form. In the structure of the solvated form of **1**, this torsion angle is 10° less, at 161°. As shown by X-ray crystallography, this crystalline form does not change to LS upon cooling to 110 K. It should be noted that in the low spin form of {Fe[HC(3,5-Me<sub>2</sub>pz)<sub>3</sub>]<sub>2</sub>}(BF<sub>4</sub>)<sub>2</sub> (**2**) observed at 173 K, the structure has a torsion angle of 179°, the angle expected for the LS form of iron(II) in this dication. Thus the failure of the solvated crystalline form of **1**, which has a much smaller average torsion angle, to undergo a spin-state change may well result from the unfavorable energetics required to dramatically change the torsion angle as well as the bond lengths. These energetic changes may well be large enough to prevent the spin-state crossover.

Both magnetic and Mössbauer spectral studies of the fragmented microcrystals that form when the single crystals of either crystalline form are taken out of solution, show that both samples are HS at ambient temperatures but change over to the LS form at low temperatures. These samples of complex **1** behave similarly to many other iron(II) complexes with an FeN<sub>6</sub> coordination environment<sup>[1]</sup> in changing completely to the LS state at low temperatures. Surprisingly, a pure sample of **1** that precipitates from the original reaction mixture changes only partially over to the LS form at low temperatures. As with the solvated, crystalline form of **1**, the energetics of the changeover are clearly different for different samples.

The behavior of complex **2** is different from that of **1** in that only half of the iron(II) sites change to LS at low temperatures, although all crystalline samples studied behave the same way. Another difference is that for **1** there is an ca. 15 degree hysteresis in the temperature dependence of the spin-state crossover, whereas no hysteresis is observed for **2**. Clearly the environment of the {Fe[HC(3,5-Me<sub>2</sub>pz)<sub>3</sub>]<sub>2</sub>}<sup>2+</sup> dication within the ionic lattice and the crystalline form influence its spin-crossover behavior.

## Experimental Section

**General Procedure:** All operations were carried out under a nitrogen atmosphere using either standard Schlenk techniques or in a

Vacuum Atmospheres HE-493 inert atmosphere dry box. All solvents were dried and distilled prior to use. Anhydrous FeI<sub>2</sub> (99.99%) was purchased from Aldrich Chemicals. Proton NMR chemical shifts are reported in ppm versus TMS. HC(3,5-Me<sub>2</sub>pz)<sub>3</sub> was prepared according to our recently reported procedures.<sup>[6]</sup> Elemental analyses were performed by Robertson Microlit Laboratories, Inc.

Magnetic susceptibilities were measured at 5 kG using a Quantum Design MPMS XL SQUID magnetometer. Gelatin capsules were used as sample containers for measurements taken in the temperature range 5–400 K. The very small diamagnetic contribution of the gelatin capsule had a negligible contribution to the overall magnetization, which was dominated by the sample. The molar magnetic susceptibilities were corrected for the diamagnetism of the complexes, which were calculated from tables of Pascal's constants to be  $-445 \times 10^{-6}$  emu/mol for {Fe[HC(3,5-Me<sub>2</sub>pz)<sub>3</sub>]<sub>2</sub>}I<sub>2</sub>.

**{Fe[HC(3,5-Me<sub>2</sub>pz)<sub>3</sub>]<sub>2</sub>}I<sub>2</sub> (1):** FeI<sub>2</sub> (0.19 g, 0.62 mmol) was dissolved in acetone (10 mL) and treated dropwise by cannula transfer with an acetone solution (10 mL) of HC(3,5-Me<sub>2</sub>pz)<sub>3</sub> (0.370 g, 1.24 mmol). The solution turned yellow and after stirring for several minutes the desired product precipitated from solution as a white powder (0.47 g, 84%), dec. 333–339 °C. The crystals used for X-ray crystallographic studies were grown by layering a saturated dichloromethane solution with hexanes and allowing the two layers to slowly combine. Two forms of the crystals, a nonsolvated form and a solvated form of the formula {Fe[HC(3,5-Me<sub>2</sub>pz)<sub>3</sub>]<sub>2</sub>}I<sub>2</sub>·4CH<sub>2</sub>Cl<sub>2</sub> (as shown by X-ray crystallography, vide infra), are produced when this crystallization procedure is repeated under seemingly identical conditions. Both forms of these crystals fragment when dried, with the solvated form losing the CH<sub>2</sub>Cl<sub>2</sub> of crystallization. Unless otherwise noted, these fragmented crystals were used in the magnetic and Mössbauer spectral studies. <sup>1</sup>H NMR (CD<sub>2</sub>Cl<sub>2</sub>): δ = −42.6 (v br, 2 H, HC), 41.1, 19.6 (v br, v br, 18 H, 18 H, Me<sub>2</sub>), 51.1 (v br, 6 H, 4-H pz). C<sub>32</sub>H<sub>44</sub>FeI<sub>2</sub>N<sub>12</sub> (906.4): calcd. C 42.40, H 4.89; found for the powder sample that precipitates from the reaction mixture: C 42.09, H 4.72; found for the nonsolvated crystalline form after drying: C 42.77, H 4.71; found for the solvated crystalline form after drying: C 42.47, H 4.78.

## X-ray Structural Data

**Nonsolvated Form of {Fe[HC(3,5-Me<sub>2</sub>pz)<sub>3</sub>]<sub>2</sub>}I<sub>2</sub>:** Colorless crystals were taken from solution and immediately coated with epoxy resin. Crystal, data collection, and refinement parameters are given in Table 3. There is no evidence of symmetry higher than triclinic, and *E*-statistics and the presence of an inversion center for the iron(II) cation suggest the centrosymmetric space group *P* $\bar{1}$  for **1**, a space group that yields a chemically reasonable and computationally stable refinement. The structure was solved using direct methods, completed by subsequent difference Fourier syntheses, and refined by full-matrix least-squares procedures. *SADABS* absorption corrections were applied to all data sets. The asymmetric unit contains half of the cationic iron(II) complex, which lies on an inversion center, and one of the iodide anions. All non-hydrogen atoms were refined with anisotropic thermal displacement coefficients. The hydrogen atom of C(1) was located from the difference map and allowed to refine, all other hydrogen atoms were treated as idealized contributions. All software and sources of the scattering factors are contained in the SHELXTL (5.10) program library (G. Sheldrick, Siemens XRD, Madison, WI).

Table 3. Crystallographic data for the structural analyses of non-solvated {Fe[HC(3,5-Me<sub>2</sub>pz)<sub>3</sub>]<sub>2</sub>}I<sub>2</sub> and Solvated {Fe[HC(3,5-Me<sub>2</sub>pz)<sub>3</sub>]<sub>2</sub>}I<sub>2</sub>·4CH<sub>2</sub>Cl<sub>2</sub>

	Nonsolvated Form	Solvated Form
Formula	C <sub>32</sub> H <sub>44</sub> FeI <sub>2</sub> N <sub>12</sub>	C <sub>36</sub> H <sub>52</sub> Cl <sub>8</sub> FeI <sub>2</sub> N <sub>12</sub>
Molecular weight	906.44	1246.15
Space group	<i>P</i> $\bar{1}$	<i>P</i> 2 <sub>1</sub> / <i>c</i>
<i>a</i> , Å	8.8062(2)	10.3214(5)
<i>b</i> , Å	10.3549(2)	12.7753(7)
<i>c</i> , Å	11.3549(2)	20.1995(11)
<i>α</i> , deg	104.0768(10)	90
<i>β</i> , deg	110.2473(10)	97.5380(10)
<i>γ</i> , deg	92.6385(11)	90
<i>V</i> , Å <sup>3</sup>	949.44(4)	2640.5(2)
<i>Z</i>	1	2
Color	colorless	colorless
ρ(calcd), g cm <sup>−3</sup>	1.585	1.567
μ(Mo- <i>K</i> <sub>α</sub> ), cm <sup>−1</sup>	20.62	18.98
Temp, K	298	190
<i>R</i> ( <i>F</i> ), <sup>[a]</sup> ( <i>wR</i> ) <sup>[a]</sup>	0.0454, 0.1186	0.0379, 0.0930

<sup>[a]</sup> Quantity minimized =  $R(wF^2) = \Sigma[w(F_o^2 - F_c^2)^2 / \Sigma w(F_o^2)^{1/2}]^{1/2}$ ;  $R = \Sigma \Delta / \Sigma (F_o)$ ,  $\Delta = |F_o - F_c|$

**Solvated Form of {Fe[HC(3,5-Me<sub>2</sub>pz)<sub>3</sub>]<sub>2</sub>}I<sub>2</sub>·4CH<sub>2</sub>Cl<sub>2</sub>:** A colorless needle was coated with inert oil, mounted on the end of a thin glass fiber and transferred to the cold stream of a Bruker SMART APEX CCD-based diffractometer system. The X-ray intensity data were measured at 190(2) K. Crystal quality and initial unit cell parameters were determined based on reflections taken from a set of three scans measured in orthogonal regions of reciprocal space. Subsequently a hemisphere of frame data was collected with a scan width of 0.3° in  $\omega$  and an exposure time of 10 s per frame. The first 50 frames were re-collected at the end of the data set to monitor crystal decay. The raw data frames were integrated into reflection intensity files with the Bruker SAINT+ program,<sup>[7]</sup> which also applied corrections for Lorentz and polarization effects. The final unit cell parameters are based on the least-squares refinement of 9412 reflections with  $I > 5\sigma(I)$  from the data set. Analysis of the data showed negligible crystal decay during data collection. An empirical absorption correction based on the multiple measurements of equivalent reflections was applied with the program SAD-ABS.<sup>[8]</sup>

{Fe[HC(3,5-Me<sub>2</sub>pz)<sub>3</sub>]<sub>2</sub>}I<sub>2</sub>·4CH<sub>2</sub>Cl<sub>2</sub> crystallizes in the space group *P*2<sub>1</sub>/*c* as determined by the systematic absences in the intensity data. The structure was solved by a combination of direct methods and difference Fourier syntheses, and refined by full-matrix least-squares against *F*<sup>2</sup>, using the SHELXTL software package.<sup>[8]</sup> The iron(II) ion is located on a special position, a center of symmetry; all other atoms are on general positions. The asymmetric unit consists of the iron(II), one HC(3,5-Me<sub>2</sub>pz)<sub>3</sub> ligand, one iodide anion and two dichloromethane molecules. All non-hydrogen atoms were refined with anisotropic thermal displacement parameters; hydrogen atoms were placed in idealized positions and refined using a riding model.

CCDC-171226 (nonsolvated form) and CCDC-171227 (solvated form) contain the supplementary crystallographic data for this paper. These data can be obtained free of charge at [www.ccdc.cam.ac.uk/conts/retrieving.html](http://www.ccdc.cam.ac.uk/conts/retrieving.html) [or from the Cambridge Crystallographic Data Center, 12, Union Road, Cambridge CB2 1EZ, UK; Fax: (internat.) +44-1223/336-033; E-mail: [deposit@ccdc.cam.ac.uk](mailto:deposit@ccdc.cam.ac.uk)].

**Mössbauer Spectroscopic Data:** The Mössbauer spectral absorber contained 47 mg/cm<sup>2</sup> of powder and the spectra were measured between 4.2 and 295 K on a constant-acceleration spectrometer which utilized a room temperature rhodium matrix cobalt-57 source and was calibrated at room temperature with an  $\alpha$ -iron foil. The estimated absolute errors are  $\pm 0.01$  mm/s for the isomer shifts,  $\pm 0.02$  mm/s for the quadrupole splittings, and  $\pm 0.5$  percent for the relative areas of the high-spin and low-spin spectral components. The relative errors are estimated to be smaller by a factor of 2 to 5.

## Acknowledgments

The authors acknowledge, with thanks, the help of Professor Hanno zur Loye and Katharine Stitzer for assistance in obtaining the magnetic data. The authors also thank the US National Science Foundation for grants CHE-0110493 to D. L. R. and DMR-9521739 to G. J. L. and the Petroleum Research Fund for grant 36368-AC3 to D. L. R. The Bruker CCD Single Crystal Diffractometer (at the University of South Carolina) was purchased with funds provided by the NSF Instrumentation for Materials Research Program through Grant DMR:9975623. F. G. thanks the “Fonds National de la Recherche Scientifique,” Brussels, Belgium for grant 9.456595 and G. J. L. thanks them for support during a sabbatical leave in Belgium.

[1] [1a] P. Gülich, in *Mössbauer Spectroscopy Applied to Inorganic Chemistry* (Ed.: G. J. Long), Plenum: New York, **1984**, Vol. 1: p 287. [1b] P. Gülich, A. Hauser, H. Spiering, *Angew. Chem. Int. Ed. Engl.* **1994**, *33*, 2024–2044. [1c] O. Kahn, J. Martinez, *Science* **1998**, *279*, 44–68.

[2] [2a] F. Grandjean, G. J. Long, B. B. Hutchinson, L. Ohlhausen, P. Neill, J. D. Holcomb, *Inorg. Chem.* **1989**, *28*, 4406–4414. [2b] G. J. Long, B. B. Hutchinson, *Inorg. Chem.* **1987**, *26*, 608–613.

[2c] J. P. Jesson, S. Trofimenko, D. R. Eaton, *J. Am. Chem. Soc.* **1967**, *89*, 3158–3164. [2d] J. P. Jesson, J. F. Weiher, S. J. Trofimenko, *Chem. Phys.* **1968**, *48*, 2058–2066. [2e] C. Cartier dit Moulin, P. Rudolf, A.-M. Flank, C.-T. Chen, *J. Phys. Chem.* **1992**, *96*, 6196–6200. [2f] C. Cartier dit Moulin, A. M. Flack, C.-T. Chen, *Jpn. J. Appl. Phys.* **1993**, *32*, Suppl. 32–2, 308–310. [2g] V. Briois, C. Cartier dit Moulin, M. Momenteau, P. Maillard, J. Zarembowitch, E. Dartyge, A. Fontaine, G. Tourillon, P. Thuéry, M. J. Verdaguer, *Chim. Phys.* **1989**, *86*, 1623–1634. [2h] N. A. Young, *J. Chem. Soc., Dalton Trans.* **1996**, 1275–1281. [2i] J.-A. Real, B. Gallois, T. Granier, F. Suez-Panama, J. Zarembowitch, *Inorg. Chem.* **1992**, *31*, 4972–4979. [2j] C. Janiak, T. G. Scharmann, T. Bräuniger, J. Holubová, M. Nádvořník, *Z. Anorg. Allg. Chem.* **1998**, *624*, 769–774.

[3] [3a] D. L. Reger, C. A. Little, A. L. Rheingold, M. Lam, T. Concolino, A. Mohan, G. J. Long, *Inorg. Chem.* **2000**, *39*, 4674–4675. [3b] D. L. Reger, C. A. Little, A. L. Rheingold, M. Lam, L. M. Liable-Sands, B. Rhagitan, T. Concolino, A. Mohan, G. J. Long, V. Briois, F. Grandjean, *Inorg. Chem.* **2001**, *40*, 1508–1520. [3c] D. L. Reger, C. A. Little, V. Young, M. Pink, *Inorg. Chem.* **2001**, *40*, 2870–2874.

[4] D. L. Reger, T. D. Wright, C. A. Little, J. J. S. Lamba, M. D. Smith, *Inorg. Chem.* **2001**, *40*, 3810–3814 and references therein.

[5] [5a] B. N. Figgis, J. Lewis, F. E. Mabbs, G. A. Webb, *J. Chem. Soc. (A)* **1967**, 442–447. [5b] G. J. Long, W. A. Baker, Jr., *J. Chem. Soc. (A)* **1971**, 2956–2959.

[6] D. L. Reger, T. C. Grattan, K. J. Brown, C. A. Little, J. J. S. Lamba, A. L. Rheingold, R. D. Sommer, *J. Organomet. Chem.* **2000**, *607*, 120–128.

[7] SMART Version 5.624, SAINT+ Version 6.02a and SADABS. Bruker Analytical X-ray Systems, Inc., Madison, Wisconsin, USA, **1998**.

[8] G. M. Sheldrick, SHELXTL Version 5.1; Bruker Analytical X-ray Systems, Inc., Madison, Wisconsin, USA, **1997**.

Received October 22, 2001

[I01417]